Pressure-induced phase transitions and electronic structure of GaAs

2008 J. Phys.: Condens. Matter 20 255204

(http://iopscience.iop.org/0953-8984/20/25/255204)

J. Phys.: Condens. Matter **20** (2008) 255204 (7pp) doi:10.1088/0953-8984/20/25/255204

Pressure-induced phase transitions and electronic structure of GaAs

D C Gupta and Subhra Kulshrestha

Condensed Matter Theory Group, School of Studies in Physics, Jiwaji University, Gwalior-474 011 (MP), India

E-mail: subhrafizix@yahoo.co.in

Received 27 February 2008, in final form 22 April 2008
Published 19 May 2008
Online at stacks.iop.org/JPhysCM/20/255204

Abstract

The structural and electronic properties of GaAs under high pressure have been investigated using an *ab initio* pseudo-potential approach within the framework of density functional theory. We use the local density approximation based on exchange–correlation energy optimization for calculating the total energy. The phase transition B3 → B1 → B2 in bulk GaAs is investigated. Results of the first-principles calculation of the structural phase transition and the electronic properties of GaAs in the three different crystallographic structures are reported. GaAs is found to undergo structural transition from B3 to B1 phase, demonstrating a reasonably good agreement with experimental data. The equation of state for these transformations also shows good agreement with experimental results. The calculated value of volume collapse is close to the observed data. The energy of the B2 phase is found to be slightly higher than that of the B1 phase. A possible mechanism for the B3 → B2 transition characterized by the space group $Pm\bar{3}m$ is discussed. The calculated values show that there is a relatively small value of enthalpy for the B3 → B1 transition as compared to the B3 → B2 transition, which provides the transition behaviour of GaAs from the kinetic viewpoint. The electronic structures have also been computed at different volumes.

(Some figures in this article are in colour only in the electronic version)

1. Introduction

The availability of higher resolution in high pressure diffraction experiments and developments in diamond anvil cell techniques have shed new light on the atomic scale mechanisms of structural phase transitions in semiconductors [1, 2]. Recently, it has become possible to compute with greater accuracy an important number of electronic and structural parameters of solids from first-principle calculations [3–8]. These developments in computer simulations have opened up many interesting and exciting possibilities in condensed matter studies. It is now possible to explain and predict properties of solids which were previously inaccessible to experiments. It gives us a clearer understanding of the theories of condensed matter and the determination of fundamental parameters. Experimental as well as theoretical studies of the structural phase transformations under pressure and of mechanical properties of materials have attracted the attention of researchers in the last few decades [9, 10].

The material GaAs belongs to the III–V group with binary octets of $A^N B^{8-N}$ type and has certain electronic properties superior to silicon. For example, it has higher saturated electron velocity and higher electron mobility, allowing it to function even at frequencies in excess of 250 GHz. It is a material recommended for circuitry in mobile phones, microwave links and radar systems. Under ambient conditions, it is a direct band gap semiconductor and hence can be used to emit light. Because of its high switching speed, it would seem to be ideal for computer applications. This material is found to have a four-fold coordinated zinc blende (B3) structure under ambient conditions. Under high pressures, it transforms to the six-fold coordinated rock salt (B1) structure followed by the eight-fold coordinated CsCl (B2) structure.

The aim of the present computation is to perform a comparative study of the structural phase transition and electronic structure of GaAs (from B3–to–B1–to–B2) by using SPHInX code based on density functional theory (DFT) by the *ab initio* pseudo-potential method. A survey of the literature reveals that earlier workers have computed either phase transformation or band/electronic structure. Not many theoretical studies of the electronic structure of GaAs in the

B2 phase are available. Hence, we thought it pertinent to study the B3 → B1 → B2 phase transformation along with the electronic structure and density of states (DOS) in different phases to study the change in band shapes, band gap and semiconductor to metal transition. This is expected to lead us to a better understanding of the interactions.

The material chosen for the present study, GaAs, shows complicated phases under high pressure. Under pressure, it transforms from the zinc blende structure (GaAs-I) into an orthorhombic phase (GaAs-II), with proposed space group $Pmm2$ [2] whose structure can be seen as a distortion of the B1 (space group $Fm\bar{3}m$) phase [3–5]. The transition pressure was about 17 GPa [2] and the latest result is 12±1.5 GPa [1]. When pressure is above 24 GPa, the diffraction pattern suggests a further transformation from GaAs-II to GaAs-III (a body-centred orthorhombic structure, with space group $Imm2$) and a gradual transformation to GaAs IV hexagonal structure in the pressure range 60–80 GPa [2] and finally to B2 phase at around 124 GPa.

Our present study is concentrated on the GaAs-I to GaAs-II transition (distorted B1 structure) which is simplified as a perfect B1 structure [6] and B3 → B2 phase transition.

This paper is organized as follows. In section 2, we briefly describe the theory used and the method of computation of parameters used in the calculations. In section 3, we discuss the calculated results on structural phase transition and electronic properties and finally the paper is concluded in section 4.

2. Theory and method of calculation

The calculations have been performed using the *ab initio* pseudo-potential approach as implemented in the SPHInX code, within the framework of DFT [11], which has been known to yield reliable results for the electronic and structural properties of materials with d-electrons. The time-independent Schrödinger equation for ions (i.e. the atomic nuclei) and electrons for a many-body wavefunction Ψ is given as:

$$H\Psi = E\Psi$$

or

$$\left(-\frac{\hbar^2}{2m_e}\sum_i \nabla_i^2 + \sum_{i,I}\frac{Z_I e^2}{|r_i - R_I|} + \frac{1}{2}\sum_{i\neq j}\frac{e^2}{|r_i - r_j|} - \sum_I \frac{\hbar^2}{2M_I}\nabla_I^2 + \frac{1}{2}\sum_{I\neq J}\frac{Z_I Z_J e^2}{|R_I - R_J|} - E\right)\psi = 0.$$

Here, the electrons are denoted by lower case subscripts and nuclei (ions) with charge Z_I and mass M_I, respectively, by upper case subscripts. The second, third and fifth terms in the above equation denote the Coulomb interactions between electrons and ions, electrons and electrons and ions and ions, respectively. Setting the mass of the ions (nuclei) as infinite, the kinetic energy of the ions (nuclei) can be ignored.

The many-body problem has been simplified using DFT, in which electronic charge density is assumed to be the fundamental variable rather than the wavefunction, i.e. it is assumed that for a given non-degenerate non-polarized ground state wavefunction, there is a unique electron density. Thus Ψ is a unique functional of the charge density, and hence the energy (E) is uniquely defined by charge density. It is a ground state theory that incorporates both exchange and correlation effects, and is computationally more efficient than the Hartree–Fock method which includes eigenvalues that do not necessarily correspond with the physical eigenvalues of the system (with the exception of the highest occupied state) as well as poor excited state modelling and hence band gap prediction.

Hohenberg and Kohn [12] proved that the total energy of a system, including that of the many-body effect of electrons (exchange and correlation) in the presence of static external potential, is a unique functional of the charge density. The minimum value of the total energy functional is the ground state energy of the system. The electronic charge density which yields the minimum is then the exact single particle ground state energy.

It was then Kohn and Sham [13] who showed that it is possible to replace the many-electron problem by an exactly equivalent set of self-consistent one-electron equations. The total energy functional can be written as a sum of several terms:

$$E[\rho(\mathbf{r})] = T_s[\rho(\mathbf{r})] + \frac{e^2}{2}\int\int \frac{\rho(\mathbf{r})\rho(\mathbf{r}')}{|\mathbf{r}-\mathbf{r}'|}\,\mathrm{d}^3\mathbf{r}\,\mathrm{d}^3\mathbf{r}' + E_{xc}[\rho(\mathbf{r})]$$

where $E_{xc}[\rho(\mathbf{r})]$ is the exchange–correlation energy. Some details are presented in the appendix.

The exchange–correlation potential is calculated using the local density approximation (LDA) [13]. In this, the exchange–correlation energy (ECE) of an electronic system is constructed by assuming that the ECE per electron at a point $\mathbf{r}$ in the electron gas $\varepsilon_{xc}(\mathbf{r})$ is equal to the ECE per electron in a homogeneous electron gas that has the same electron density at the point $\mathbf{r}$. It follows that

$$E_{xc}^{LDA}[\rho(\mathbf{r})] = \int \varepsilon_{xc}^{hom}[\rho(\mathbf{r})]\rho(\mathbf{r})\mathrm{d}^3\mathbf{r}.$$

Therefore, the exchange potential in LDA

$$v^{LDA}[\rho(\mathbf{r})] = \frac{\delta E_{xc}^{LDA}[\rho(\mathbf{r})]}{\delta\rho(\mathbf{r})} = \frac{\delta\left[\int \rho(\mathbf{r})\varepsilon_{xc}^{hom}\rho(\mathbf{r})\right]}{\delta\rho(\mathbf{r})} = \varepsilon_{xc}^{hom}[\rho(\mathbf{r})] + \frac{\delta\varepsilon_{xc}^{hom}[\rho(\mathbf{r})]}{\delta\rho(\mathbf{r})}\rho(\mathbf{r}).$$

2.1. Determination of the total energy and theoretical equilibrium lattice constant

The total energy (E) is calculated by a self-consistent run and can be expressed as the sum of the kinetic energy of electrons, self-energy, Hartree energy, electrostatic energy, local pseudo-energy, non-local energy, exchange–correlation energy, exchange–correlation potential energy and screening energy.

The lattice constant of a solid corresponds to the size of the conventional unit cell length at the equilibrium volume and is obtained computationally by minimizing the total energy as a function of cell volume. We have performed several calculations of the total energy for various lattice constants and obtained the value of lattice constant for which the total

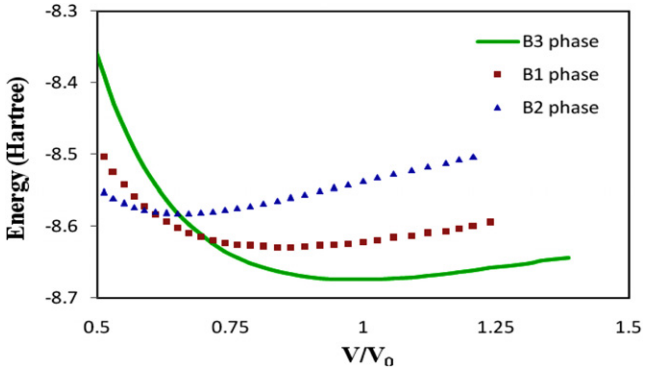

Figure 1. The variation of energy (hartree per unit cell/atom) versus reduced volume for various structures of GaAs.

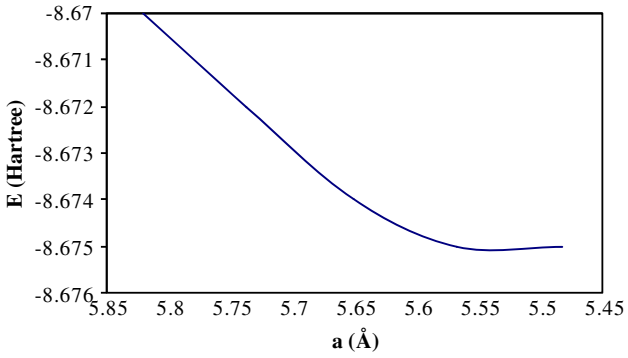

Figure 2. Total energy (E) versus lattice constant (a) for GaAs in the parent phase (B3).

energy becomes minimal. The calculation of lattice constant is straightforward for cubic systems—it is performed at several different volumes using the same energy cut-off and k-point sampling.

The results are fitted to the Murnaghan equation of state

$$P(V) = \frac{B_0}{B_0'}\left[\left(\frac{V_0}{V}\right)^{B_0'} - 1\right].$$

Here, B_0 is the equilibrium bulk modulus and B_0' its first pressure derivative. Here the pressure (P) is the negative derivative of the total energy

$$P = -\frac{\partial E}{\partial V}.$$

Therefore, B_0 effectively measures the curvature of the energy versus volume curve at the relaxed volume (V_0).

$$B_0 = -V\left(\frac{\partial P}{\partial V}\right)_T \qquad \text{and} \qquad B_0' = \left(\frac{\partial B_0}{\partial P}\right)_T.$$

Norm-conserving non-local pseudo-potentials [14] were constructed for Ga^{3+} and As^{5+} ions using the method of Hamann [15] and the pseudo-potentials include scalar relativistic effects.

A mesh of 4 × 4 × 4 special k-points is taken in the whole Brillouin zone for all three phases and a cut-off energy of 24 Ryd for B1 and B3 phases and of 34 Ryd for the B2 phase is taken. Both the plane wave cut-off and the number of k-points were varied to ensure total energy convergence.

3. Results and discussion

GaAs at ambient pressure crystallizes in the zinc blende (B3 phase) structure and undergoes a transition to the rock salt (B1 phase) structure upon compression. Besides, it also transforms to CsCl (B2 phase) structure at very high pressures. In this work, we analyse all the three structures using the LDA. The total energies, calculated as a function of volume ($Å^3$) are reported in figure 1. The curves are obtained by fitting the calculated values to Murnaghan's equation of state [16]. In this graph, the volume is expressed in terms of the theoretical zero pressure volume of the B3 phase $V_{0,\text{theor}}^{\text{GaAs}}$ (42.97 $Å^3$).

Table 1. Values of the calculated lattice parameter (a, in Å), the bulk modulus (B_0, in GPa) and its pressure derivative (B_0') at equilibrium volume for B3, B1 and B2 phases and the Ga–As distance (in Å) in the B1 phase at transition pressure (P_T) of GaAs.

a	B_0	B_0'	Ga–As distance at P_T	Reference
		GaAs in B3 phase		
5.56	79.75	3.50	—	Present work
5.65	74.8	4.49	—	Expt [17, 18]
5.51	82.1	—	—	Others [4]
6.41	—	—	—	Others [10]
		GaAs in B1 phase		
5.28	69.95	4.87	2.47	Present work
	—	—	2.48	Expt [1]
		GaAs in B2 phase		
4.80	50.30	5.84	—	Present work

It is seen from this figure that the results obtained by us are in good agreement with the results obtained by Garcia and Cohen [4] (who have employed similar theory to calculate these properties) and better than those obtained by Singh and Singh [10] for the B3 → B1 phase transition of GaAs. The energy of the B1 phase is higher than that of the B3 phase while that of the B2 phase is higher than the energy of the B1 phase which is the criterion for the relative stability of the competitive phases.

Results for the convergence of energy with respect to lattice constant are shown in figure 2. It is found that the convergence occurs close to the experimental lattice constant. This correct description of lattice constant shows that the interaction considered in the present formulation is capable of predicting correctly the minimum free energy of GaAs in the B3 phase.

The corresponding equilibrium lattice parameter in B3, B1 and B2 phases as well as the bulk modulus B_0 and its pressure derivative B_0' are listed along with the corresponding experimental values [17] and values computed by others [4, 10] in table 1. Since GaAs occurs in the B3 phase in ambient conditions, which is the parent phase, and its B_0 is comparatively higher than that of compressed B1 and B2 phases, it indicates compression in all the three directions of

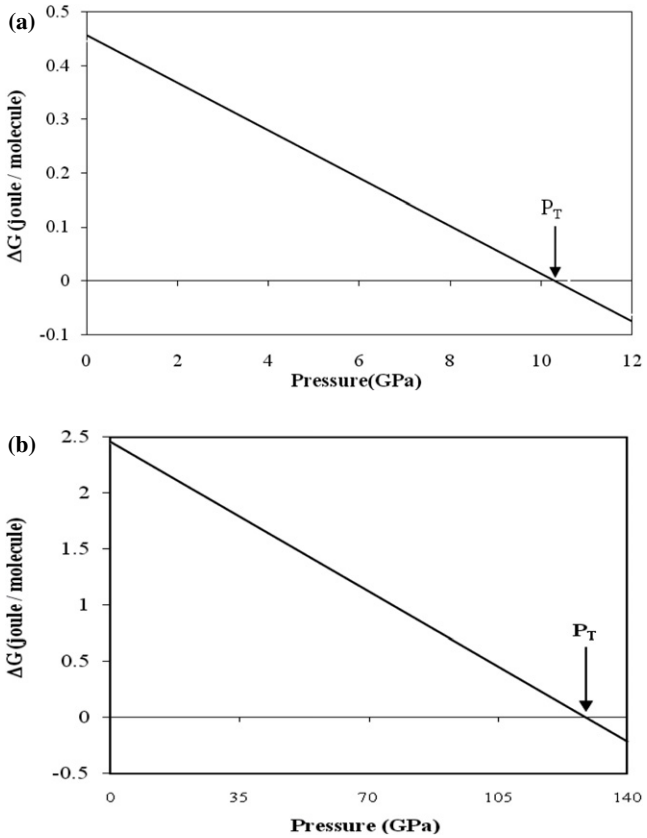

Figure 3. Variation of the Gibbs free energy difference (ΔG) with pressure (P): (a) for B3 $\rightarrow$ B1 transformation and (b) for the B3 $\rightarrow$ B2 transformation in GaAs.

bulk GaAs. Due to compression, the ions rearrange themselves to minimize the Gibbs free energy for hypothetical structures.

To determine the phase transition pressure at $T = 0$ K (i.e. the entropy of the crystal is ignored) the Gibbs free energy ($G = E + PV$) of B3, B1 and B2 phases is calculated at different pressures. The pressures at which ΔG ($= G_{B1} - G_{B3}$ and $G_{B2}-G_{B3}$) becomes zero is called the phase transition pressure (P_T). The B3 $\rightarrow$ B1 and B3 $\rightarrow$ B2 phase transition pressures are calculated using the LDA scheme. The Gibbs free energy difference (ΔG) thus obtained is plotted as a function of pressure (P) in figures 3(a) and (b). The pressure corresponding to ΔG approaching zero is P_T and is indicated by the arrows in these figures.

It is clear from figure 1 and table 2 that at zero pressure, the B3 phase is a thermodynamically stable state of GaAs because the computed Gibbs free energy is found to be a minimum, which is in agreement with the experimental results and remains stable until the pressure reaches a value of about 10.5 GPa. It is also clear from this table that the values of ΔE for B3 $\rightarrow$ B1 and B3 $\rightarrow$ B2 phases are positive, which is a necessary condition for the stability of the two competitive phases. As pressure increases beyond the phase transition pressure ($P_T = 10.5$ GPa for B1 phase and 128.8 GPa for B2 phase, respectively), the phase at which free energy becomes more negative will become thermodynamically stable. At pressures above 10.5 GPa, the B3 phase becomes thermodynamically unstable while

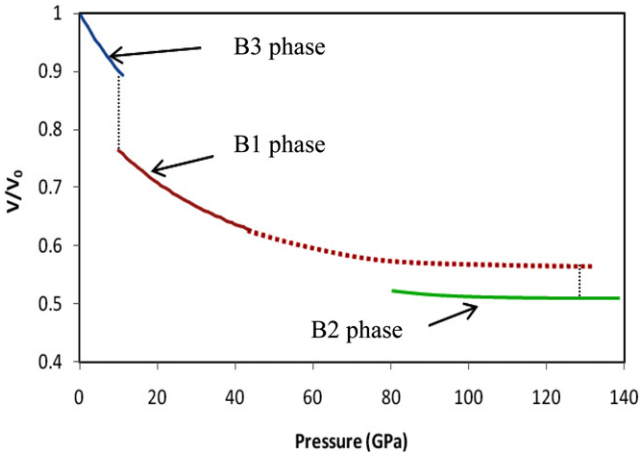

Figure 4. Phase diagram of GaAs where dotted ($\cdots\cdots$) lines are the extrapolated data of the B1 phase.

Table 2. Calculated values of the phase transition pressure (P_T, in GPa) for B3 $\rightarrow$ B1 and B3 $\rightarrow$ B2 phases, volume collapse (%) at phase transition pressure, energy of the structures at zero pressure with respect to that of the B3 phase $\Delta E = \{(E_{Hypo} - E_{0(B3\ phase)})$ in hartree per unit cell/atom} and volume (V_0, in Å^3) of GaAs. The results are also compared with the available experimental and other theoretical data.

	B3 $\rightarrow$ B1	B3 $\rightarrow$ B2	Reference
P_T	10.5	128.8	Present work
	12 ± 1.5	—	Expt [1]
	12.3	—	[6]
	11.8	—	[4]
	17.0	—	[10]
	16.0	—	[19]
	26.7	—	[9]
	—	∼124	[7]
$\Delta V(P)/V(0)$	13.8	—	Present work
	14.0	[10]	

	B3 phase	B1 phase	B2 phase	
ΔE	0.00	0.05	0.10	Present work
V_0	42.97	36.80	27.65	Present work
	45.17	—	—	Expt [20]

the B1 phase remains stable and the B2 phase seems to be stable above 128.8 GPa.

To understand the mechanism of the transformation of a semiconductor to other phases, we have plotted the variation of the relative volume $V(P)/V(0)$ with pressure (P) in figure 4 computed from the Murnaghan equation of state [16] as

$$\frac{V}{V_0} = \left(1 + \frac{B_0'}{B_0}P\right)^{-1/B_0'}.$$

It is clear from figure 4 that the volume changes smoothly up to 10.5 GPa. At this pressure, an abrupt decline of volume is seen. After 10.5 GPa, volume decreases gradually and at 128.8 GPa another change of volume is obtained, beyond this and up to 200 GPa no sharp modification of volume is seen. The magnitude of the discontinuity in volume at the transition pressure is obtained from the phase diagram shown in figure 4 and its values are tabulated in table 2.

3.1. Electronic properties

To understand the change in the nature of the bands, we have calculated the total density of states (TDOS) and band structure at the LDA level of theory for GaAs along the directions of high symmetry in four different structures or densities, i.e. in (i) B3 phase at zero pressure; (ii) B3 phase just before the B3 → B1 phase transition; (iii) B1 phase just after the B3 → B1 phase transition; (iv) B2 phase just after the B1 → B2 phase transition. The overall band profiles are in fairly good agreement with previous results [8, 21].

Under ambient conditions, GaAs is stable in the B3 phase having a semiconducting gap produced by the arrangement of electrons into the bonding orbital. In figure 5(a), the valence band maximum (VBM) and conduction band minimum (CBM) occur at the Γ point. Thus, the energy gap is direct with a value of about 0.9 eV, while the experimental value is 1.45 eV. The band gap is underestimated in comparison with experimental results. This underestimation of the band gap is mainly due to the fact that the simple form of LDA does not take into account the quasi-particle self-energy correctly [22] which makes it not sufficiently flexible to accurately reproduce both exchange-correlation energy and its charge derivative. It is noted that the density functional formalism is limited in its validity [23] and the band structure derived from it cannot be used directly for comparison with experiments. The conduction band of GaAs follows the same trend; these bands arise from Ga 'd'-like states with a little contribution from 'p'-like states of As-atom. The lowest lying band arises from 's'-like states of the As-atom. The upper valence bands which lie above this band are mainly due to 'p'-like states of the As-atom with the top occurring at the Γ point.

It is clear from figure 5(b) that at the Γ point, the top of the valence band rises up to the Fermi level and at the X point the bottom of the conduction band drops in energy and lies down near the Fermi level. Hence, it seems to become an indirect band gap (Γ → X) of about 0.58 eV. When we increase the pressure, the B1 phase compresses (figure 5(b)) and the bonding region becomes smaller. Therefore, kinetic energy of the electrons in the bond increases and the energy difference between the valence band and conduction band decreases. The behaviour of the lowest conduction band at the X point shows this change. It is localized in the octahedral region between the anions and as the volume is compressed, the state drops in energy and reduces the band gap. Therefore, at high pressures, the B3 phase would be metallic. However, before this can occur, the crystal transforms into other structures. The gap which makes the B3 phase stable at low pressures is responsible for the instability at high pressures.

The band structure and the density of states for GaAs in the B1 phase (just after the B3 → B1 phase transition) are shown in figure 5(c). It is clear from this figure that there is a well-developed gap at the Fermi level (the same as that of the B3 phase). But the conduction band at the X point lies below the valence band maximum at the Γ point and this makes the B1 phase metallic.

The pressure dependence at the X point in the B1 phase is opposite to the behaviour in the B3 phase. It is clearly seen from figures 5(a) and (b) that as the pressure increases the band

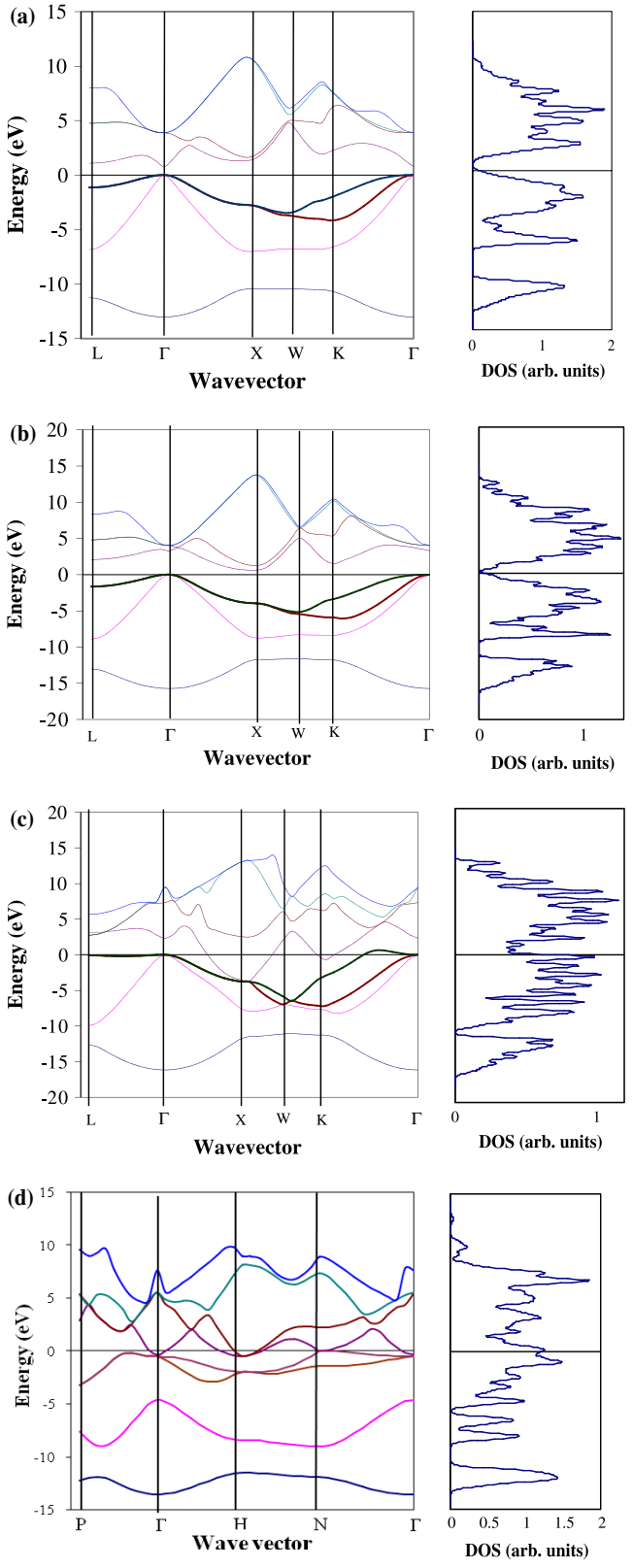

Figure 5. (a) Band structure and DOS of GaAs in the B3 phase at zero pressure. (b) Band structure and DOS of GaAs in the B3 phase just before the B3 → B1 phase transition. (c) Band structure and DOS of GaAs in the B1 phase just after the B3 → B1 phase transition. (d) Band structure and DOS of GaAs in the B2 phase just after the B1 → B2 phase transition.

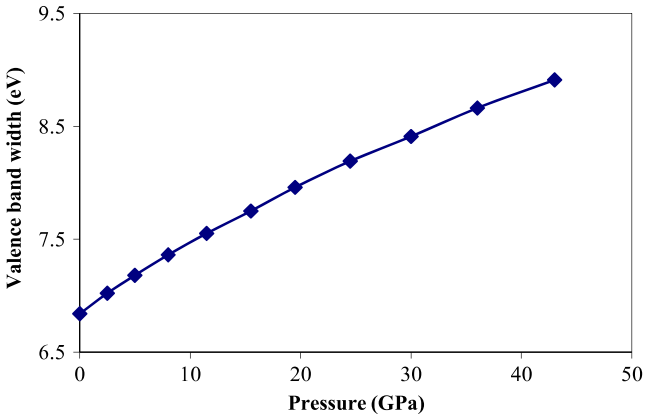

Figure 6. Valence bandwidths as a function of pressure in the B3 phase of GaAs.

overlap in the B3 phase increases but from figure 5(c) the band overlap decreases with increase in pressure in the B1 phase.

The band structure and the DOS of GaAs in the B2 phase (just after the B1 → B2 phase transition) are shown in figure 5(d). It is clear from this figure that at the Γ point the conduction band lies below the Fermi level but still there is a gap of about 0.16 eV, but at the *N* point the top of the valence band overlaps with the conduction band. Hence at the *N* point, band overlap metallization occurs. The metallization is due to band broadening with the increase in pressure and subsequent overlap of the filled valence (the p-like valence band of the anion) and the conduction band (the d-like conduction band of the cation).

It is clear from the DOS at different volumes that as the volume decreases the small side peaks start growing throughout the energy range, which clearly shows that these changes in the DOS may be responsible for a phase transformation from four- to six-fold structure. It is also clear from the DOS of B3 and B2 phases (figures 5(a) and (d)), that the 's'-like band has the same shape and size with a minor change in peak height, hence we can say that the 's'-band does not participate actively in phase transformation.

The dependence of the valence bandwidth (VBW) on hydrostatic pressure for GaAs with B3 phase is shown in figure 6. It is clear from this figure that VBW increases with increase in pressure from 0 to 50 GPa. This suggests that there is a decrease of the ionicity character of GaAs under hydrostatic pressure.

4. Conclusion

We have used the LDA within the pseudo-potential method to study the structure and electronic properties at normal as well as high pressure phases of GaAs. The structural parameters, phase transition pressure and volume collapse are found to be in good agreement with experimental and previous theoretical results. The energy band gap under ambient conditions in the B3 phase has been calculated and it is slightly less than the experimental value. The pressure dependence of the valence bandwidth is also investigated and shows a reasonable explanation for the ionic character of GaAs.

Acknowledgments

The authors are grateful to the University Grant Commission, New Delhi for financial support. One of us (SK) is also grateful to UGC, New Delhi for the award of fellowship. We thank Professor Abdallah Hammoudeh Qteish, Yarmouk University, Jordan for fruitful suggestions. The authors would also like to thank Professors (Dr) J Neugebauer, Martin Fuchs and S Boeck, FHI-Berlin, Germany for providing the SPHInX code.

Appendix

Appendix.1 Hohenberg–Kohn theorem

(1) $\mathrm{v}(\mathbf{r}) \overset{1-1}{\longleftrightarrow} \rho(\mathbf{r})$
gives the one-to-one correspondence between external potentials $v(\mathbf{r})$ and ground state densities $\rho(\mathbf{r})$.

(2) Variational principle
Given a particular system characterized by the external potential $v_0(\mathbf{r})$, the solution of the Euler–Lagrange equation

$$\frac{\delta}{\delta\rho(\mathbf{r})}E_{\mathrm{HK}}[\rho] = 0$$

yields the exact ground state energy E_0 and ground state density $\rho_0(\mathbf{r})$ of this system

(3) $E_{\mathrm{HK}}[\rho] = F[\rho] + \int \rho(\mathbf{r})v_0(\mathbf{r})\,\mathrm{d}^3r$
$F[\rho]$ is universal and expressed as $F[\rho] = F^{(0)}[\rho] + e^2F^{(1)}[\rho] + e^4F^{(2)}[\rho] + \cdots$ where: $F^{(0)}[\rho] = T_s[\rho]$ (kinetic energy of non-interacting particles)

$$e^2F^{(1)}[\rho] = \frac{e^2}{2}\int\int \frac{\rho(\mathbf{r})\rho(\mathbf{r}')}{|\mathbf{r}-\mathbf{r}'|}\,\mathrm{d}^3\mathbf{r}\,\mathrm{d}^3\mathbf{r}' + E_x[\rho]$$

(Hartree + exchange energies)

$$\sum_{i=2}^{\infty}(e^2)^i F^{(i)}[\rho] = E_{\mathrm{c}}[\rho] \qquad \text{(correlation energy)}$$

$$\Rightarrow F[\rho] = T_s[\rho] + \frac{e^2}{2}\int\int \frac{\rho(\mathbf{r})\rho(\mathbf{r}')}{|\mathbf{r}-\mathbf{r}'|}\mathrm{d}^3\mathbf{r}\,\mathrm{d}^3\mathbf{r}' + E_x[\rho] + E_{\mathrm{c}}[\rho].$$

Appendix.2 Kohn–Sham equations

Mapping of the interacting many-electron system onto a system of non-interacting electrons moving in an effective potential due to the other electrons means that we can write the Schrödinger equation for an electron in the non-interacting system as:

$$\left[-\tfrac{1}{2}\nabla^2 + \mathrm{v}_{\mathrm{eff}}(\mathbf{r})\right]\psi_i(\mathbf{r}) = \varepsilon_i\psi_i(\mathbf{r}) \qquad i = 1, 2, \ldots, N$$

where $\mathrm{v}_{\mathrm{eff}}(\mathbf{r}) = \mathrm{v}_0(\mathbf{r}) + \mathrm{v}_{\mathrm{H}}[\rho(\mathbf{r})] + \mathrm{v}_{\mathrm{xc}}[\rho(\mathbf{r})]$ therefore,

$$\left[-\tfrac{1}{2}\nabla^2 + \mathrm{v}_0(\mathbf{r}) + \mathrm{v}_{\mathrm{H}}[\rho(\mathbf{r})] + \mathrm{v}_{\mathrm{xc}}[\rho(\mathbf{r})]\right]\psi_i(\mathbf{r}) = \varepsilon_i\psi_i(\mathbf{r})$$

where Hartree potential $\mathrm{v}_{\mathrm{H}}[\rho(\mathbf{r})] = \int \frac{\rho(\mathbf{r}')}{|\mathbf{r}-\mathbf{r}'|}\,\mathrm{d}^3\mathbf{r}'$;

The exchange correlation potential, $v_{xc}[\rho(\mathbf{r})] = \frac{\delta E_{xc}[\rho(\mathbf{r})]}{\delta\rho(\mathbf{r})}$ with the electronic density of N electrons

$$\rho(\mathbf{r}) = \sum_{i=1}^{N} |\psi_i(\mathbf{r})|^2.$$

The wavefunctions $\Psi_i(\mathbf{r})$ are called the Kohn–Sham orbitals.

References

[1] Besson J M, Itie J P, Polian A, Weill G, Mansot J L and Gonzalez J 1991 *Phys. Rev.* B **44** 4214
[2] Weir S T, Vohra Y K, Vanderborgh C A and Ruoff A L 1989 *Phys. Rev.* B **39** 1280
[3] Mujica A, Rubio A, Munoz A and Needs R J 2003 *Rev. Mod. Phys.* **75** 863
[4] Garcia A and Cohen M L 1993 *Phys. Rev.* B **47** 6751
[5] Rino J P, Chatterjee A, Ebbsio I, Kalia R K, Nakano A, Shimojo F and Vashishta P 2002 *Phys. Rev.* B **65** 195206
[6] Cai J, Chen N and Wang H 2007 *J. Phys. Chem. Solids* **68** 445–57
[7] Mujica A, Needs R J and Munoz A 1995 *Phys. Rev.* B **52** 8881
[8] Froyen S and Cohen M L 1983 *Phys. Rev.* B **28** 3258
[9] Chelikowsky J R 1987 *Phys. Rev.* B **35** 1174
[10] Singh R K and Singh S 1989 *Phys. Rev.* B **39** 671
[11] Hohenberg P and Kohn W 1964 *Phys. Rev.* B **136** 864
[12] Hohenberg P and Kohn W 1965 *Phys. Rev.* **137** A1697
[13] Kohn W and Sham L J 1965 *Phys. Rev.* **140** 1133
[14] Hamann D, Schluter M and Chiang C 1979 *Phys. Rev. Lett.* **43** 1494
[15] Hamann D R 1989 *Phys. Rev.* B **40** 2980
[16] Murnaghan F D 1944 *Proc. Natl Acad. Sci. USA* **305** 390
[17] Weast R C 1970 *Handbook of Chemistry and Physics* 62nd edn (Boca Raton, FL: CRC Press) pp E99–103
[18] Martin R M 1970 *Phys. Rev.* B **1** 4005
[19] Zhang S B and Cohen M L 1987 *Phys. Rev.* B **35** 7604
[20] Madelung O (ed) 1966 *Elastic, Piezoelectric, Piezooptic, and Electrooptic Contants of Crystals* (*Landolt-Bornstein New Series* vol 1 Group III) (Berlin: Springer)
[21] Demkov A A, Sankey O F, Gryko J and McMillan P F 1997 *Phys. Rev.* B **55** 6904
[22] Rashkev S N and Lambrecht W R L 2001 *Phys. Rev.* B **63** 165212
[23] Onida G, Reining L and Rubio A 2002 *Rev. Mod. Phys.* **74** 601